Experimental Demonstration of Symmetrical Waveform Generation Based on Amplitude-Only Modulation in a Fiber-Based Temporal Pulse Shaping System

Ming Li, *Member, IEEE*, Yichen Han, *Student Member, IEEE*, Shilong Pan, *Member, IEEE*, and Jianping Yao, *Senior Member, IEEE*

***Abstract*—We experimentally demonstrate the photonic generation of symmetrical waveforms based on amplitude-only modulation in a fiber-based temporal pulse shaping (TPS) system. A rectangular waveform with a 3-dB width of 18.8 ps and a triangular waveform with a 3-dB width of 6.7 ps are experimentally generated.**

***Index Terms*—Amplitude-only modulation, symmetrical waveform generation, temporal pulse shaping (TPS).**

I. Introduction

ULTRASHORT optical waveforms in the picosecond or subpicosecond regime could find applications in numerous fields such as ultrafast optical communications, medical imaging, and coherent control in chemistry [1]. Due to the limited sampling speed of the state-of-the-art digital electronics, the speed of currently available electronic arbitrary waveform generation systems is limited to 10 Gb/s [2]. Thanks to the inherent high speed and broadband width offered by modern optics, the generation of ultrafast arbitrary waveforms in the optical domain based on optical pulse shaping has been a topic of interest recently.

Ultrafast optical waveforms can be generated based on pulse shaping using a spatial light modulator (SLM). The major advantage of using an SLM for ultrafast pulse shaping is that an SLM can be updated in real time [3], [4], making the system reconfigurable with large flexibility. The major limitations of an SLM-based pulse shaping system are its large size, poor stability and high loss due to the implementation involving free-space optics.

Optical waveform generation can also be implemented based on pure fiber optics, which offers the advantages such as smaller size, lower loss, better stability and higher potential for integration [5]–[8]. Among the different techniques, the one based on spectral shaping and wavelength-to-time (SS-WTT) mapping is particularly suitable for optical waveform generation based on pure fiber optics [5], [6]. The generation of a chirped microwave waveform based on SS-WTT mapping has been recently reported [5], [6]. A major limitation of this technique, however, is the poor reconfigurability, since the spectral response of the optical spectral shaper is hard to be tuned once the filter is fabricated.

Optical arbitrary waveforms can also be generated in the time domain based on temporal pulse shaping (TPS) [7]–[9]. In a TPS system, two conjugate dispersive elements are connected before and after an optical modulator. The waveform at the output of the TPS system is a Fourier-transformed version of the modulation signal, which can be used to generate a fast waveform using a relatively slow waveform. The same concept has also been used to implement microwave spectrum analysis [10]. The key advantage of the TPS technique is that a high-speed pulse can be generated using a relatively low-speed waveform. The major difficulty of the approach is that the input waveform is usually complex valued, and the modulation of a complex-valued waveform requires an intensity modulator and a phase modulator with precise synchronization. It is interesting to note, based on the Fourier transform property, a symmetrical waveform has a Fourier transform that is always real. Based on this fact, Haner and Warren proposed to generate arbitrary symmetrical waveforms using a TPS system implemented based on free-space optics [9]. With the rapid development of fiber optics, a TPS system can be practically realized based on pure fiber-optics. A TPS system based on pure fiber-optics was proposed by Chi and Yao in [7], but the technique was studied numerically with no experimental demonstration performed due to the lack of an arbitrary waveform generator (AWG) at that time. In this letter, an experimental demonstration of a purely fiber-based TPS system for the generation of symmetrical waveforms is presented. A rectangular waveform with a 3-dB width of 18.8 ps and a triangular waveform with a 3-dB width of 6.7 ps are experimentally generated.

II. Principle and Experimental Setup

Fig. 1 shows the TPS system for the generation of a symmetrical waveform. A transform-limited Gaussian pulse is generated by a mode-locked laser (MLL). The transform-limited Gaussian pulse can be expressed as $g(t) = \exp\left(-t^2/\tau_0^2\right)$,

Manuscript received October 30, 2010; revised March 04, 2011; accepted March 16, 2011. Date of publication March 24, 2011; date of current version May 13, 2011. This work was supported by the Natural Sciences and Engineering Research Council of Canada (NSERC).

The authors are with the Microwave Photonics Research Laboratory, School of Information Technology and Engineering, University of Ottawa, Ottawa, ON K1N 6N5, Canada (e-mail: jpyao@site.uOttawa.ca).

Color versions of one or more of the figures in this letter are available online at http://ieeexplore.ieee.org.

Digital Object Identifier 10.1109/LPT.2011.2132122

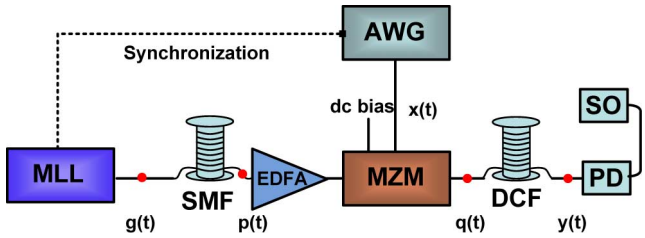

Fig. 1. Experimental setup. MLL: Mode-locked laser. PD: Photodetector. AWG: Arbitrary waveform generator. MZM: Mach–Zehnder modulator. EDFA: Erbium-doped fiber amplifier. SMF: Single-mode fiber. DCF: Dispersion-compensating fiber. SO: sampling oscilloscope.

where τ_0 is the half pulse width at $1/e$ maximum. Its Fourier transform is given by $G(\omega) = \sqrt{\pi}\tau_0 \exp\left(-\tau_0^2\omega^2/4\right)$, where ω denotes the angular frequency. Two conjugate dispersive elements, connected before and after the MZM, are a single-mode fiber (SMF) and a dispersion compensating fiber (DCF). An erbium-doped fiber amplifier (EDFA) is connected before the MZM to compensate for the optical loss in the SMF. The transfer functions of the SMF and the DCF are given by $H_{SMF}(\omega) = \exp\left(j\ddot{\Phi}_{SMF}\omega^2/2\right)$ and $H_{DCF}(\omega) = \exp(j\ddot{\Phi}_{DCF}\omega^2/2)$, where $\ddot{\Phi}_{SMF}$ and $\ddot{\Phi}_{DCF}$ are the group velocity dispersion (GVD) of the SMF and the DCF, respectively. Since the dispersion of the two dispersive elements are matched, we have $\ddot{\Phi}_{SMF} = -\ddot{\Phi}_{DCF}$.

The optical signal after the EDFA is then directed into the MZM which is operating in a push-pull mode. Mathematically, when a continuous-wave $\exp(j\omega_0 t)$, where ω is the angular frequency, ω_0 is introduced to an MZM, the electric field $e_{IM}(t)$ of the modulated signal at the output of the push-pull MZM is given by $e_{IM}(t) = \exp(j\omega_0 t)\times\{\exp[-j\beta x(t)]+\exp[j\beta x(t)+ j\phi_0]\}$, where β is the phase modulation index, ϕ_0 is a static phase shift introduced by the dc bias and $x(t)$ denotes the modulation signal. To perform temporal spectrum shaping with a real signal that has both positive and negative values [7], the MZM is biased at the minimum transmission point with a dc bias voltage to introduce a π phase shift (i.e., $\phi_0 = \pi$) between the two arms of the MZM. $e_{IM}(t)$ can then be approximated to be $e_{IM}(t) \approx \exp(j\omega_0 t) \times \{-2j\sin[\beta x(t)]\}$. Therefore, the amplitude modulation function $m(t)$ when the MZM is biased at the minimum transmission point is $m(t) = -2j\sin[\beta x(t)]$. The optical signal at the output of the DCF is given by [10]

$$y(t) = C \times \exp\left(j\frac{t^2}{2\ddot{\Phi}_{DCF}}\right) \times \Im\left\{G\left(\frac{t}{\ddot{\Phi}_{SMF}}\right) \times m(t)\right\}\Big|_{\omega=t/\ddot{\Phi}_{DCF}}, \quad (1)$$

where $\Im$ denotes the Fourier transform, and C is a constant. If the optical signal at the output of the DCF is applied to a photodetector (PD), we have the output current, given by

$$I(t) = \Re\,|y(t)|^2 = 4\Re C^2 \times \left\{\Im\left[G\left(\frac{t}{\ddot{\Phi}_{SMF}}\right) \times \sin\left[\beta x\left(t\right)\right]\right]\Big|_{\omega=t/\ddot{\Phi}_{DCF}}\right\}^2, \quad (2)$$

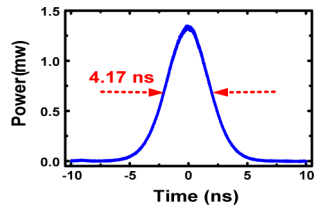

Fig. 2. Measured optical pulse at the output of the SMF.

where $\Re$ is the responsivity of the PD. Based on (2), to generate a waveform $I(t)$, the modulation signal should be

$$x(t) = \frac{1}{\beta} \times \arcsin\left\{\frac{1}{2C\sqrt{\Re}} \frac{\Im^{-1}\left[\sqrt{I(t)}\right]\Big|_{\omega=t/\ddot{\Phi}_{DCF}}}{G\left(\frac{t}{\ddot{\Phi}_{SMF}}\right)}\right\}, \quad (3)$$

where $\Im^{-1}$ denotes the inverse Fourier transform. It can be seen from (3) that the input modulation signal can be calculated based on the target waveform and the optical waveform at the output of the SMF. When the target output waveform $I(t)$ is a symmetrical waveform, the inverse Fourier transform of $\sqrt{I(t)}$ is real. Thus, the target symmetrical waveform can be generated based on a TPS system with amplitude-only modulation.

III. Experiment

An experiment is performed based on the setup shown in Fig. 1. An ultrashort optical pulse train from the MLL with a repetition rate of 48.6 MHz is sent to the SMF. The individual pulse in the pulse train has a 3-dB temporal width of 550 fs. A SMF with GVD of -784.24 ps^2 is employed to temporally stretch the optical pulse. The GVD of the DCF is matched to that of the SMF which is 784.24 ps^2. Since the optical waveform at the output of the DCF is a scaled version of the Fourier transform of the optical waveform at the output of the MZM, it can be seen from (3) that the input modulation signal $x(t)$ can be calculated based on the optical waveform $G(t/\ddot{\Phi}_{SMF})$ at the output of the SMF and the target output waveform $I(t)$. Therefore, the impact of the finite temporal width of the input optical pulse on the shape of the generated waveform can be eliminated. The modulation signal $x(t)$ is generated by an AWG. The synchronization between the AWG and the MLL is realized by externally locking the clock of the AWG with one of the harmonic frequencies of the pulse train from the MLL. The optical waveform $G(t/\ddot{\Phi}_{SMF})$ can be measured by a high-speed photodetector (PD) and an oscilloscope at the output of the SMF. Fig. 2 shows the measured optical waveform at the output of the SMF which has a 3-dB temporal width of 4.17 ns.

When the target output $I(t)$ is a rectangular waveform, the optical signal at the output of the MZM should be a sinc waveform. Based on (3), the input modulation signal can be obtained, as shown in Fig. 3(a). Mathematically, the width of the main lobe of the sinc waveform is 6.67 ns, which should result in a rectangular waveform with a width 24.00 ps at the output of the DCF. The spectrum of the optical signal at the output of the MZM is measured by an optical spectrum analyzer (OSA), as shown in Fig. 3(b). Since the optical pulse from the MLL is transform-limited and Gaussian, after the SMF the pulse is linearly stretched, and the stretched pulse should have a shape that

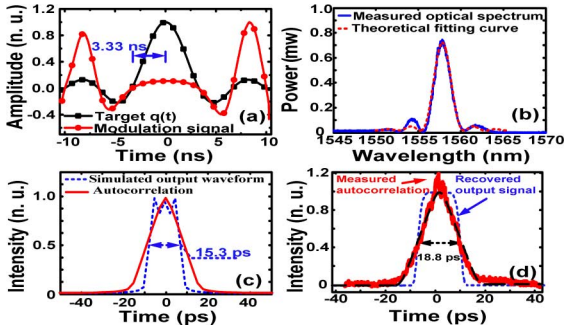

Fig. 3. (a) Target optical waveform at the output of the MZM and the calculated modulation signal. (b) Measured spectrum of the optical signal at the output of the MZM and its fitting curve with the square of a sinc function. (c) Simulated waveform at the output of the DCF and its autocorrelation. (d) Measured autocorrelation (solid line) at the output of the DCF, the recovered waveform (dotted line) from the measured optical autocorrelation, and its simulated autocorrelation (dashed line).

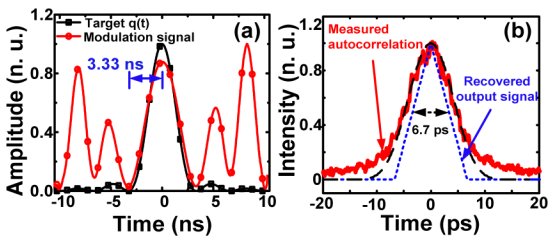

Fig. 4. (a) Target optical waveform at the output of the MZM and the calculated input modulation signal. (b) Measured autocorrelation (solid line) at the output of the DCF, the recovered waveform (dotted line) from the measured optical autocorrelation, and its simulated autocorrelation (dashed line).

is Gaussian both in the frequency domain and in the temporal domain. Therefore, we can use the optical spectrum at the output of the MZM to evaluate the temporal waveform. As can be seen from Fig. 3(b), the optical waveform at the output of the MZM is a sinc function.

For the DCF, if the input waveform is a sinc function, the output should be a rectangular waveform. Fig. 3(c) shows the calculated waveform at the output of the DCF, which is a rectangular wave with a 3-dB width of 15.3 ps. The ripples on the top of the rectangular waveform are caused by the truncation of the sinc waveform at the MZM. Since the output waveform is too fast to detect using a PD, an autocorrelator is employed to measure the output waveform. It is known that the autocorrelation of a rectangular waveform is triangular. The measured autocorrelation output and the recovered output signal (i.e., the rectangular waveform) are shown in Fig. 3(d). As can be seen a triangular waveform is observed. Based on the autocorrelation output, we calculate the width of the experimentally generated rectangular waveform, which is 18.8 ps. A good agreement between the simulated and the experimental results is reached.

To verify the programmability of the TPS system, a new input modulation signal is applied to generate a triangular waveform. Similar to the generation of the rectangular waveform, we should first calculate the modulation signal. It is known, to generate a triangular waveform, the waveform at the output of the MZM should be the square of a sinc function. In the experiment, the width of the main lobe of the waveform at the output of the MZM is 6.67 ns, and thus the 3-dB width of the simulated triangular waveform at the output of the DCF is 6.00 ps. Fig. 4(b) shows the measured autocorrelation output at the output of the DCF, the recovered signal from the autocorrelation output is a triangular waveform with a 3-dB width of 6.7 ps. Again, a good agreement is reached.

IV. Discussion and Conclusion

Note that if the two dispersive elements are not perfectly mismatched in dispersion, the system can equivalent to the TPS system with two dispersive elements that are perfectly matched in dispersion, and followed by a third dispersive element. Although, a waveform is perfectly generated at the output of the second dispersive element, it is stretched by the third dispersive element, leading to a distorted output waveform. In addition, compared with a TPS system that could generate any arbitrary waveforms, the proposed system can only generate symmetrical waveforms. Since the implementation is greatly simplified, it can still find applications where symmetrical waveforms are needed.

It is known that the speed of currently available electronic AWGs is limited to 10 Gb/s, one approach to improving the temporal resolution of the system is to increase the dispersion of the dispersive element. However, as shown in Fig. 1, when the dispersion of the SMF is too large, any two adjacent optical pulses at the output of the SMF after time stretching will overlap. Therefore, there exists a trade-off between pulse repetition rate and the temporal resolution of the system.

In summary, we have experimentally demonstrated the generation of symmetrical waveforms based on amplitude-only modulation in a purely fiber-based TPS system. A rectangular waveform with a 3-dB width of 18.8 ps and a triangular waveform with a 3-dB width of 6.7 ps were generated.

References

[1] A. M. Weiner, "Femtosecond optical pulse shaping and processing," *Prog. Quantum Electron.*, vol. 19, no. 3, pp. 161–237, 1995.

[2] Tektronix AWG7000 Series Arbitrary Waveform Generators [Online]. Available: http://www.tek.com/products/signal_sources/awg7000/index.html

[3] A. M. Weiner, "Femtosecond pulse shaping using spatial light modulators," *Rev. Sci. Instrum.*, vol. 71, no. 5, pp. 1929–1960, May 2000.

[4] J. D. McKinney, D. E. Leaird, and A. M. Weiner, "Millimeter-wave arbitrary waveform generation with a direct space-to-time pulse shaper," *Opt. Lett.*, vol. 27, no. 15, pp. 1345–1347, Aug. 2002.

[5] H. Chi and J. P. Yao, "All-fiber chirped microwave pulse generation based on spectral shaping and wavelength-to-time conversion," *IEEE Trans. Microw. Theory Tech.*, vol. 55, no. 9, pp. 1958–1963, Sep. 2007.

[6] C. Wang and J. P. Yao, "Chirped microwave pulse compression using a photonic microwave filter with a nonlinear phase response," *IEEE Trans. Microw. Theory Tech.*, vol. 57, no. 2, pp. 496–504, Feb. 2009.

[7] H. Chi and J. P. Yao, "Symmetrical waveform generation based on temporal pulse shaping using an amplitude-only modulator," *Electron. Lett.*, vol. 43, no. 7, pp. 415–417, Mar. 2007.

[8] S. Thomas, A. Malacarne, F. Fresi, L. Poti, A. Bogoni, and J. Azaña, "Programmable fiber-based picosecond optical pulse shaper using time-domain binary phase-only linear filtering," *Opt. Lett.*, vol. 34, no. 4, pp. 545–547, Feb. 2009.

[9] M. Haner and W. S. Warren, "Synthesis of crafted optical pulses by time domain modulation in a fiber-grating compressor," *Appl. Phys. Lett.*, vol. 52, no. 18, pp. 1458–1460, May 1988.

[10] R. E. Saperstein, D. Panasenko, and Y. Fainman, "Demonstration of a microwave spectrum analyzer based on time-domain processing in fiber," *Opt. Lett.*, vol. 29, no. 5, pp. 501–503, Mar. 2004.

[11] M. A. Muriel, J. Azana, and A. Carballar, "Real-time Fourier transformer based on fiber gratings," *Opt. Lett.*, vol. 24, no. 1, pp. 1–3, Jan. 1999.